Electronic and transport properties of perfect sp^2-bonded amorphous graphitic carbon

Ming-Zhu Huang and W. Y. Ching
Department of Physics, University of Missouri–Kansas City, Kansas City, Missouri 64110
(Received 13 September 1993)

The electronic and transport properties of a perfect amorphous graphitic carbon model constructed by Townsend *et al.* [Phys. Rev. Lett. **69**, 921 (1992)] are studied by first-principles calculations within the local-density approximation. It is shown that such a random system with two-dimensional interaction in a three-dimensional structure is a high-resistivity metal. A zero-temperature resistivity of about 1160 $\mu\Omega$ cm and a positive thermopower at low temperature are obtained. Localized states near the Fermi level are induced by subtle difference in the π bonding of different ring structures. Relaxation time due to elastic electron-electron scattering and the Fermi velocity are estimated to be 2.4×10^{-15} s and 2.61×10^{4} m/s, respectively.

I. INTRODUCTION

The physics of noncrystalline solids continues to attract a great deal of experimental and theoretical attention.[1] It is now quite well established that the dimensionality of the system plays an important role in the properties of the disordered solids.[2] In this regard, dimensionality usually refers to specific interactions related to the structure of the solid. While real three-dimensional (3D) noncrystalline solids are quite common, such as in amorphous semiconductors or in metallic glasses, two-dimensional (2D) systems are generally approximated by atoms absorbed on surfaces or layered compounds in which the interlayer interactions can be neglected. Examples of the latter include He on graphite surfaces,[3] graphite intercalation compounds,[4] antiferromagnets on 2D triangular or Kagome lattices realized in $SrCr_{8-x}Ga_{4+x}O_{19}$,[5,6] etc. For theoretical studies, idealized models can be constructed for both 3D and 2D disordered systems.

Recently, Townsend *et al.*[7] constructed a random schwarzite model of amorphous graphitic carbon. The model is a part of the result in studying periodic carbon structures with minimal surface and a negative Gaussian curvature (NGC).[8–11] Ordinary graphite surface, with all six-membered rings (MR), has a zero Gaussian curvature. Fullerene systems and related fullerene tubules have positive Gaussian curvature by having five MR. NGC models are obtained by introducing seven and/or eight MR. The amorphous graphitic model of Townsend *et al.* contains random fractions of five, six, seven, and eight MR in forming a network of 2D sheets with no broken bonds and therefore has both positive and negative Gaussian curvatures. The model is in the form of a fcc lattice with $a=42.92$ Å and contains a total of 1248 C atoms (mass density $=1.268$ g/cm^2). The distributions of the bond length and bond angle of the model show very small distortions from the corresponding values in graphite as indicated in Fig. 1. The average bond length (bond angle) is 1.420 Å (119.81°) with a standard deviation of only 0.014 Å (9.32°). Our analysis of the model shows it has 380 five MR, 2998 six MR, 365 seven MR, and only 1 eight MR. Beeman *et al.* had actually hand built a threefold-bonded 1120-atom cluster of *a*-C and analyzed its radial-distribution function (RDF).[12] The Beeman model has a significantly larger bond angle and bond-length distortions.

The Townsend model is highly interesting because it represents an ideal model to study weak localization in a random system with 2D bonding in a 3D structure. It is different from the low-density graphite fibers, which consist of hexagonal honeycomb arrays of graphene planes containing many defects.[13] The disorder in the Townsend model, which contains large voids of open compartments, arises strictly from minor topological variations rather than from impurities. The model is sufficiently large that the effect of having a periodic boundary is

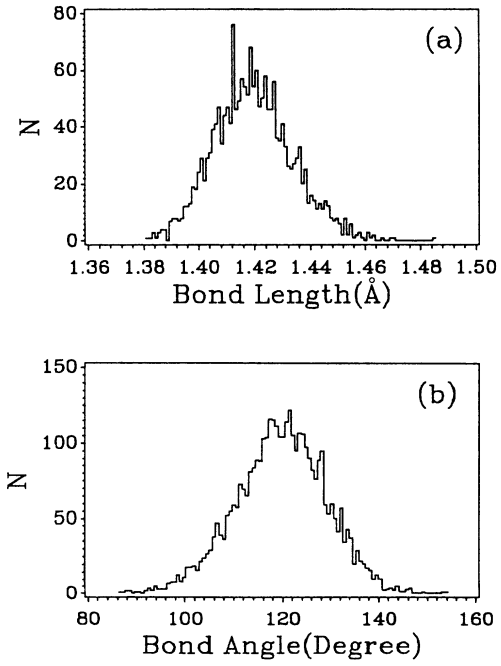

FIG. 1. Distribution of (a) bond lengths and (b) bond angles in the Townsend model.

0163-1829/94/49(7)/4987(6)/$06.00

negligible. Although the real *a*-C materials may contain a substantial portion of sp^3 tetrahedral bonding,[14] or even some twofold C-C bonding,[15] the calculated RDF of the Townsend model seems to agree well with *a*-C film grown by sublimation,[7] indicating that such a structure may be realizable in real materials. It has been pointed out that a random graphitic structure with large pores is easier to form than crystalline schwarzite structures with a NGC, although the stabilities of the two are similar.[7] In fact, many naturally occurring substances such as zeolites, biomembranes, and certain proteins[16] have 2D bonding structures. It has also been suggested that the tip region in the growth of C nanotubes may contain amorphous graphiticlike layers.[17] Nevertheless, in the context of the present study, we regard the Townsend model as an ideal model structure for a disordered system, and use it to study the microscopic properties of such a system.

In this paper, we present the results of a detailed *ab initio* calculation of the electronic, optical, and transport properties of the Townsend model, and show some very surprising results. We find the system to be metallic with a finite density of states (DOS) at the Fermi level. Localized states exist not necessarily only at the band edges, but can be induced by subtle differences in the π bonding of different ring structures. We have obtained a zero-temperature resistivity of 1160 $\mu\Omega$ cm; a positive temperature coefficient at low temperature. At low frequency, the optical conductivity follows a Drude-type behavior characteristic of a metal.

II. METHOD OF CALCULATION

We use the first-principles orthogonalized linear combination of atomic orbitals method (OLCAO) in the local-density approximation to calculate the electronic structure and use the resulting wave functions for studying the transport and the optical properties. The method has been applied to fcc C_{60},[18–20] alkali metal-doped C_{60},[21–24] and a large number of NGC graphitic models.[25,26] The computational details have been sufficiently described before and we will give only a brief outline. Specifically, the basis function consists of atomic orbitals centered at each C atom in the model. The valence Bloch sums of the C 2*s* and C 2*p* are properly orthogonalized to the C 1*s* core. The atom-centered potential function is obtained from the self-consistent calculation of the fcc C_{60} as described before.[18] Both the atomic basis functions and the potential functions are expressed as linear combinations of Gaussian-type orbitals, which facilitates the analytic evaluation of interaction matrix elements, including the momentum matrix elements to be used in the optical and transport properties calculations. Interactions between all of the atoms are included although contributions from the sixth and seventh nearest neighbors become negligibly small.

The scale of *ab initio* calculation with a model of 1248 atoms is computationally very demanding. We take full advantage of the economic use of the basis orbitals in the OLCAO method in accomplishing such a calculation. The full diagonalization of the matrix equation including overlap of size 4992×4992 yields all the energy eigenvalues and wave functions necessary for the transport properties calculation. Also, because the Townsend model is sufficiently large, it suffices to calculate only at the center of the mini-quasi-Brillouin zone.

III. RESULTS ON ELECTRONIC STRUCTURE

Figure 2(a) shows the calculated DOS of the model. The zero of the energy scale is set at the Fermi level E_F, which has a DOS value $N(E_F)$ of 0.098 states/eV atom. The occupied bandwidth is 21.5 eV, close to fullerence and related systems.[18,20] The main feature of the DOS is a major σ-binding peak centered at -9.0 eV and two minima, at -14 and -0.5 eV. Comparing with the DOS of crystalline graphite shown in Fig. 2(b) calculated using the same method, we see substantial differences, although the minimum at the Fermi level in the DOS of the Townsend model is close to the zero gap of graphite (lower by less than 0.3 eV). The main peak of the valence band (VB) in the graphite is at -8.0 eV, about 1 eV closer to the VB edge than the Townsend model. The VB width in graphite is about 20 eV with a rather sharp edge at -20 eV. Interestingly, the minimum at -14 eV occurs at the same place as in the Townsend model. There is no resemblance of the DOS in the conduction-band (CB) region between graphite and the Townsend model in the CB region up to 10 eV.

In Fig. 2(c), we separate the DOS of the Townsend

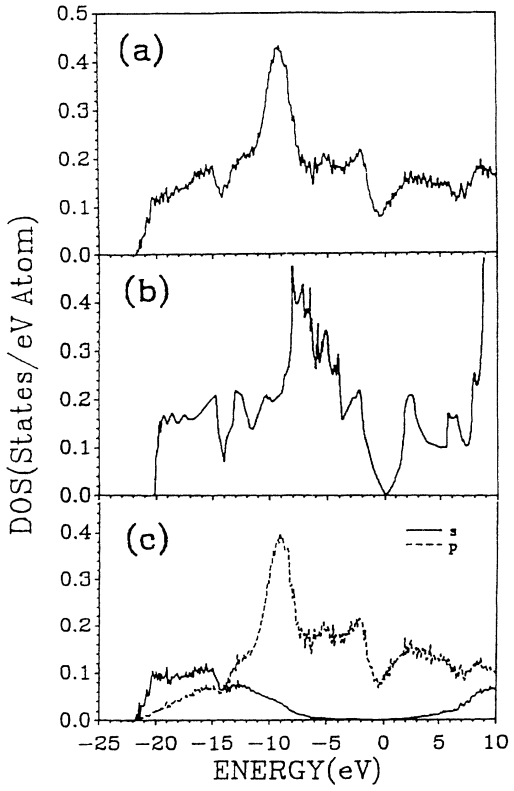

FIG. 2. Calculated DOS of (a) the Townsend model; (b) crystalline graphite; (c) orbital-projected partial DOS of (a), C 2*s*, solid line; C 2*p*, dashed line.

model into the C $2s$ and C $2p$ orbital components. As is well known, the upper portion of the VB is dominated by the π band of the $2p$ orbital states, while the lower portion is mainly from the C $2s$ orbital states. The crossover is at -14 eV. Thus, it becomes clear that the minimum at -14 eV in the DOS of both the graphite and the Townsend model is the signature of the crossover of the $2p$ and the $2s$ bands.

Figure 3 shows the partial DOS per atom of the five, six, and seven MR in the Townsend model. The partial DOS (PDOS) of different ring structures are obtained by first resolving the DOS into 1248 atomic components using the Mulliken scheme,[27] and then recombining them according to their participation in different ring structures. There are significant differences in the location of minima and maxima in these PDOS. Most conspicuous is the appearance of additional peaks at -20, -6.0, and -2.0 eV in the PDOS of five MR. This reflects the subtle difference in the sp^2 bonding of C atoms in different ring structures. The calculated average effective charges per C atom are found to be 4.086, 3.992, and 3.978 electrons per C atom in the five, six, and seven MR, respectively. Since C atoms in the five MR have greater distortion, our calculated effective charges seem to suggest that electrons prefer a more disordered environment.

Figure 4 shows the localization index I^L, or the inverse participation ratio of all the states across the entire energy range calculated from the wave functions and the overlap integrals. The localization index is calculated according to

$$I_m^L = \sum_i \left[\sum_j C_{im}^* C_{jm} S_{ij} \right]^2 , \tag{1}$$

where C_{im} is the eigenvector coefficient for the state m and S_{ij} is the overlap matrix. Relatively localized states are found in regions centered around -21, -6.0, 0, and $+7.0$ eV. The presence of localized states near the band edge at -21 eV is not surprising since this is in accordance with the formal theory of Anderson.[28] Their appearance at other locations warrants further investigation. In Fig. 5, we plot I^L of Fig. 4 in a more refined scale together with the difference spectra of the PDOS of

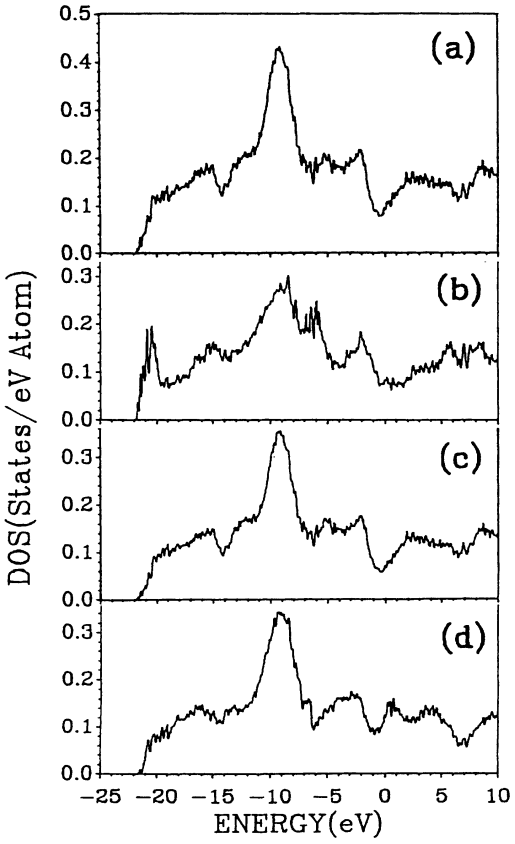

FIG. 3. Calculated DOS and PDOS per atom of the C_{1248} Townsend model: (a) total; (b) in five MR; (c) in six MR; and (d) in seven MR.

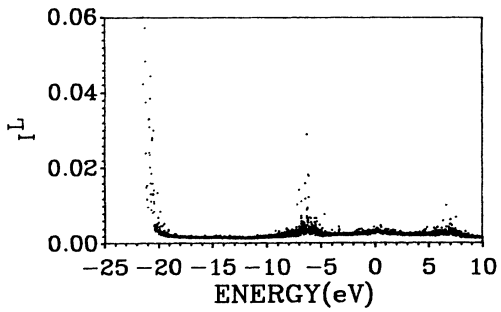

FIG. 4. Localization index for the states in the Townsend model.

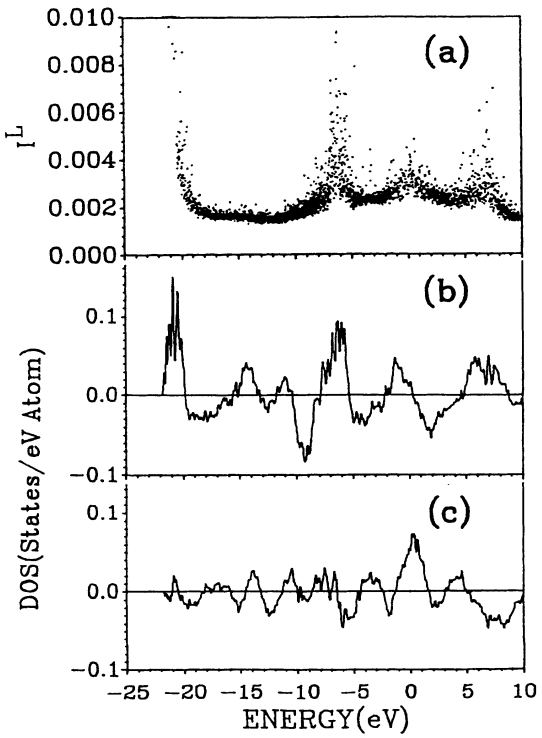

FIG. 5. (a) Localization index for the states in C_{1248} Townsend model in a more refined scale. Difference in the PDOS per atom between (b) five MR and six MR; (c) seven MR and six MR.

five MR and the seven MR from that of the six MR. Deviations from the baseline in Figs. 5(b) and 5(c) indicate the region of substantial change in the electronic structure due to different ring structures. It is quite apparent that the regions of localized states coincide with the regions where the PDOS of five MR and seven MR deviate from that of six MR the most. We therefore conclude that relatively localized states within a broadband region can be induced by subtle differences in electronic bonding in this disordered system; and such differences can probably only be delineated with first-principles calculation in which interactions between all pairs of atoms are included. This conclusion is also consistent with the fact that C atoms in the five MR have slightly large effective charges due to greater disorder. Alternatively, one may argue that the large localization for states near -6 and $+7$ eV is because these states are at the edges of the σ bands. This interpretation is not inconsistent with the notion that bonding differences between various ring structures is mostly reflected in the states at the edge of the σ band.

IV. RESULTS ON OPTICAL AND TRANSPORT PROPERTIES

With both the electronic states and wave functions for the Townsend model calculated, it is possible to study transport and optical properties of the system. The first step is to calculate an energy-dependent conductivity function $\sigma(E)$ according to the Kubo-Greenwood formula,[29]

$$\sigma(E)=\frac{2\pi\hbar e^2}{3m^2\Omega}\sum_{i,j}|\langle i|\mathbf{p}|j\rangle|^2\delta(E_1-E)\delta(E_j-E)\ . \quad (2)$$

The double δ functions in (1) describe the scattering of an electron with energy E_i to a state with energy E_j. The quantum-mechanical nature of the scattering is all contained in the momentum matrix elements $\langle i|\mathbf{p}|j\rangle$. Because the model is finite, the energy eigenstates are discrete. To satisfy the double δ functions in (1), it is necessary to broaden each eigenstate to obtain a continuous spectrum. The size of broadening is inversely proportional to the number of atoms in the model. In our case, a Gaussian broadening of 0.04 eV was applied to each state in the evaluation of $\sigma(E)$. At low temperature, only the $\sigma(E)$ near E_F is important and its value at E_F gives the zero-temperature conductivity, or resistivity, $\rho(0)=1/\sigma(E_F)$. The calculated $\sigma(E)$ near E_F is shown in Fig. 6. The conductivity curve has a negative slope at E_F, and a zero-temperature conductivity value of 0.86×10^{-4} $(\mu\Omega\,\mathrm{cm})^{-1}$, or equivalently, a resistivity value of 1160 $\mu\Omega$ cm at 0 K and 1235 $\mu\Omega$ cm at 91 K. This value is comparable to that of semimetals such as gray tin ($\rho=2000$ $\mu\Omega$ cm at 91 K) and bismuth ($\rho=106.5$ $\mu\Omega$ cm at 273 K),[30] and is about five times that of fluorine-intercalated graphite fibers.[31] The high-resistivity value is obviously related to the localized states near the Fermi level shown in Fig. 2(a).

Figure 7 shows the calculated optical dielectric function $\varepsilon_2(\omega)$, using the same transition matrix elements as in Eq. (1). Because of the large number of states involved, only transitions for photon energy up to 2.0 eV

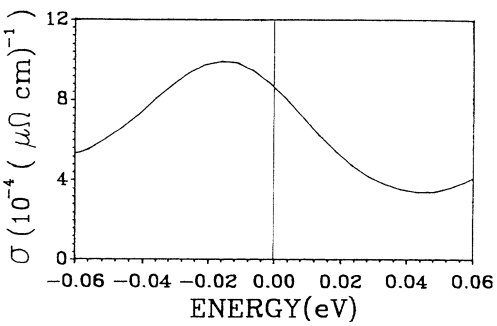

FIG. 6. Calculated dc conductivity function near the Fermi level.

are considered. In a large unit-cell calculation for amorphous solids, there is no distinction between interband and intraband transitions.[32] If we assume the system to be free-electron-like, we may fit $\varepsilon_2(\omega)$ at low frequency to the Drude expression in the relaxation-time approximation[33]

$$\varepsilon_2(\omega)=[\omega_p^2\tau]/[\omega(1+\omega^2\tau^2)]\ , \quad (3)$$

where ω_p is the plasmon frequency and τ is the relaxation time. ω_p can be estimated from the peak of the electron-energy-loss function, $\mathrm{Im}[1/\varepsilon(\omega)]$. We have calculated the energy-loss function by obtaining the real part of the dielectric function from the imaginary part by Kramers-Kronig transformation. The calculated energy-loss function is shown in the inset of Fig. 7 with a broad peak at $\hbar\omega_p=1.54$ eV. Using this value for ω_p and by fitting the calculated $\varepsilon_2(\omega)$ to Eq. (3), we obtain a relaxation time τ for conduction electrons in such a system to be of the order of 2.4×10^{-15} s. We can also estimate the Fermi velocity $v_F=(\partial E_F/\partial\mathbf{k})/\hbar$ for the conduction electrons. This is done by approximating the partial differential as the finite difference in the Fermi energy. The electronic structure calculation for the Townsend model is repeated at $\mathbf{k}=\pi/a[1,1,1]$, where a is the size of the model lattice. We obtain $\mathbf{v}_F=2.61\times10^4$ m/s. Combining with the relaxation time τ obtained above, we estimate the electron mean free path in the Townsend model to be $l=\tau v_F=0.63$ Å. This is a quite resonable number, show-

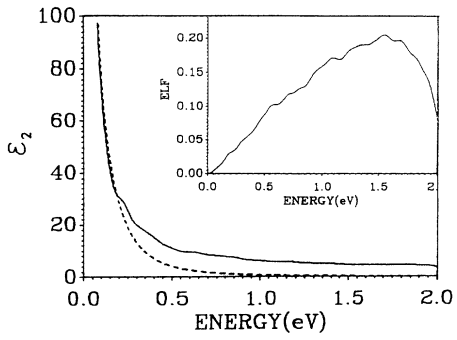

FIG. 7. Calculated imaginary dielectric function. The dashed line is the Drude model. Inset shows the energy-loss function obtained from the complex dielectric function.

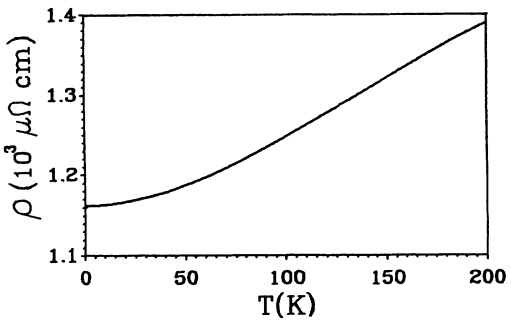

FIG. 8. Calculated temperature-dependent resistivity of the Townsend model.

ing the conduction electron in such a disordered system is scattered quite strongly. While the above estimation may be subject to some uncertainty for reasons to be stated below, we emphasize that the present calculation does not invoke any parameters such as carrier density and effective mass, which are difficult to determine. Estimation of $\mathbf{k}_F$ from $\mathbf{v}_F$ leads to a value of 1.44 for $l\mathbf{k}_F$ which indicates the material to be in the range of weak localization.[1]

From the computed $\sigma(E)$ curve, we may estimate the low-temperature behavior of resistivity $\rho(T)$ and thermopower $s(T)$ according to the standard expressions

$$\rho(R)=1/\sigma(0,T)=\left[\int\left[-\frac{\partial f(E)}{\partial E}\right]\langle\sigma(E)\rangle dE\right]^{-1} \tag{4}$$

and

$$S(T)=[1/\sigma(0,t)]\frac{K}{e}\int\langle\sigma(E)\rangle\frac{E-E_F}{KT}\frac{\partial f(E)}{\partial E}dE\ . \tag{5}$$

The results of these calculations are shown in Figs. 8 and 9, respectively. It shows that at low temperature, the material should have a positive temperature coefficient and the thermopower will rise steadily from zero to a maximum of about 28 (μV/K) at about 126 K. The slope for the initial linear $S(T)$ is 0.42 μV/K^2. The low-temperature $S(T)$ value is similar to fluorine-intercalated graphite,[31] which is also considered to be a weak localization system.

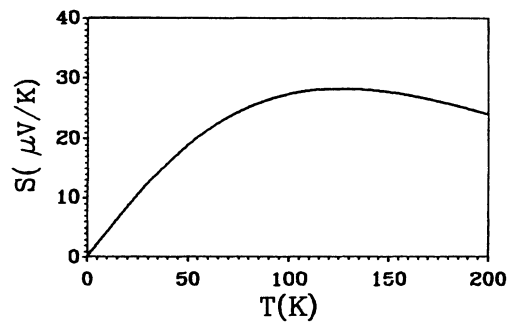

FIG. 9. Calculated thermopower of the Townsend model at low temperature.

V. DISCUSSION

We must caution that the above results for the transport properties of the Townsend model are qualitative at best for the following reasons. First, Eqs. (2), (4), and (5) consider only elastic electron-electron scattering. Although the effect of disorder is fully accounted for, the effect of electron-phonon interaction and other types of inelastic scattering has been neglected. Second, the present calculation is based on local-density theory and it is not clear whether this theory is adequate for *e-e* interaction. Third, whether the Drude model is applicable to the conduction electron system in the Townsend model is also not clear. And last, configurational average $\langle\cdots\rangle$ in the calculation of $\sigma(E)$ should be taken over several independent models. Since the Townsend model itself is sufficiently large in size, and the broadening of the eigenstate spectrum is reasonably small, we believe our results based on a single model are still qualitatively valid.

In spite of the above concerns, we believe the present work provides a computationally tractable way of studying transport properties of disordered solids. Previously, this approach has been applied to the study of transport properties of metallic glasses with considerable success,[32,34] even though the model structures are much smaller. Allen and Broughton used a similar approach to study electric conductivity of liquid Si.[35] An empirical LCAO method was used. Because of the difficulty in estimating the optical matrix within the tight-binding scheme, the results on the optical and transport properties were inconclusive. The present first-principles approach should be able to provide more accurate and conclusive results.

It is also interesting to compare the electronic properties of the Townsend model with that of the Vanderbilt-Tersoff (VT) model of negative-curvature fullerene.[10] VT had constructed a 168-atom fullerene model with a NGC in the form of a fcc lattice. The electronic structure and the optical properties of the VT C_{168} model have been calculated by us using the same method. The VT model turns out to be a semiconductor with an indirect gap of 0.47 eV. Other than the position of the main peak, which should be similar for all sp^2-bonded C structures, the DOS of the VT C_{168} model, which is characterized with many minigaps in the VB region, is quite different from the Townsend model. The optical properties of the two models are drastically different as it should be for insulating and metallic systems. This indicates that the topological disorder introduced in the Townsend model has a profound effect on the overall electronic and optical properties of the system, notwithstanding that the local short-range order of sp^2 bonding is the same.

In conclusion, we have studied the electronic and transport properties of a "perfect" amorphous graphitic carbon described by the Townsend model. The model represents a random physical system with a 2D interaction in a 3D structure. Our first-principles microscopic calculation shows the system to be metallic, and localized

states can be induced by slight variation in the planar bonding structure. The low-temperature conductivity for such a system is comparable to common semimetals and a positive temperature coefficient of resistivity is obtained. It is conceivable that such a low-density, high-strength graphitic material can accommodate other types of atoms and molecules in its open compartments. With a possible charge-transfer mechanism to increase the carrier density, entirely different material properties with potential applications may result. We hope this work will lead to further studies on similar noncrystalline systems. Many of them may occur in nature, such that a much deeper understanding about their microscopic properties can be achieved.

ACKNOWLEDGMENTS

One of us (W.Y.C) would like to thank Tom Lenosky for providing us with the coordinates of the Townsend model. We also would like to thank Computer Services at the University of Missouri–Kansas City for making special arrangements for executing large memory jobs. This work was supported by the U.S. Department of Energy under Grant No. DE-FG02-84ER45170.

[1]See, for example, N. F. Mott and E. A. Davis, *Electronic Process in Noncrystalline Materials* (Clarendon, Oxford, 1979); also, *Localization, Interaction and Transport Phenomena,* edited by B. Kramer, G. Bergmann, and Y. Bryseraede, Springer Series in Solid State Sciences Vol. 61 (Springer, New York, 1985).

[2]P. W. Anderson, E. Abrahams, and T. V. Ramakrishnan, Phys. Rev. Lett. **43**, 718 (1979); P. A. Lee and T. V. Ramakrishnan, Rev. Mod. Phys. **57**, 287 (1985).

[3]V. Elser, Phys. Rev. Lett. **62**, 2405 (1989).

[4]*Graphite Intercalatoin Compounds II, Transport and Electronic Properties,* edited by H. Zabel and S. A. Solin, Springer Series in Materials Science Vol. 18 (Springer-Verlag, New York, 1992).

[5]R. R. P. Singh and D. A. Huse, Phys. Rev. Lett. **68**, 1766 (1992).

[6]A. P. Ramirez, G. P. Espinosa, and A. S. Cooper, Phys. Rev. Lett. **64**, 2070 (1990).

[7]S. J. Townsend, T. J. Lenosky, D. A. Muller, C. S. Nichols, and V. Elser, Phys. Rev. Lett. **69**, 921 (1992).

[8]A. L. Mackay and H. Terrones, Nature **355**, 762 (1991).

[9]T. Lenosky, X. Gonze, M. Teter, and V. Elser, Nature **355**, 333 (1992).

[10]D. Vanderbilt and J. Tersoff, Phys. Rev. Lett. **68**, 511 (1992).

[11]M. O'Keeffe, G. B. Adams, and O. F. Sankey, Phys. Rev. Lett. **68**, 2325 (1992).

[12]D. Beeman, J. Silverman, R. Lynds, and M. R. Anderson, Phys. Rev. B **30**, 870 (1984).

[13]M. S. Dresselhaus and M. Endo, in *Graphite Intercalation Compoiunds II, Transport and Electronic Properties* (Ref. 4), p. 347.

[14]J. Robertson, Adv. Phys. **35**, 317 (1986).

[15]C. Z. Wang, K. M. Ho, and C. T. Chan, Phys. Rev. Lett. **70**, 611 (1993).

[16]S. Anderson, S. T. Hyde, K. Larsson, and S. Lidin, Chem. Rev. **88**, 221 (1988).

[17]R. E. Smalley, Mater. Sci. Eng. B (to be published).

[18]W. Y. Ching, M.-Z. Huang, Y.-N. Xu, W. G. Harter, and F. T. Chan, Phys. Rev. Lett. **67**, 2045 (1991).

[19]W. Y. Ching, M.-Z. Huang, Y.-N. Xu, and F. Gan, Mod. Phys. Lett. B **6**, 309 (1992).

[20]Y.-N. Xu, M.-Z. Huang, and W. Y. Ching, Phys. Rev. B **46**, 4241 (1992).

[21]Y.-N. Xu, M.-Z. Huang, and W. Y. Ching, Phys. Rev. B **44**, 13 171 (1991).

[22]M.-Z. Huang, Y.-N. Xu, and W. Y. Ching, J. Chem. Phys. **96**, 1648 (1992).

[23]Y.-N. Xu, Z.-Z. Huang, and W. Y. Ching, Phys. Rev. B **46**, 6572 (1992).

[24]M.-Z. Huang, Y.-N. Xu, and W. Y. Ching, Phys. Rev. B **47**, 8249 (1993).

[25]W. Y. Ching, M.-Z. Huang, and Y.-N. Xu, Phys. Rev. B **46**, 9910 (1992).

[26]M.-Z. Huang, W. Y. Ching, and T. L. Lenosky, Phys. Rev. B **47**, 1593 (1993).

[27]R. S. Mulliken, J. Am. Chem. Soc. **23**, 1833 (1955).

[28]P. W. Anderson, Phys. Rev. **109**, 1492 (1952).

[29]D. A. Greenwood, Proc. Phys. Soc. London **71**, 585 (1960).

[30]*Numerical Data and Functional Relationship in Science and Technology,* edited by O. Madelung, M. Schulz, and H. Weiss, Landolt-Börnstein, New Series, Vol. 17 (Springer-Verlag, New York, 1982).

[31]L. Piraux *et al.*, Phys. Rev. B **41**, 4961 (1990).

[32]G.-L. Zhao, Yi He, and W. Y. Ching, Phys. Rev. B **42**, 10 887 (1990).

[33]J. M. Ziman, *Principles of the Theory of Solids* (Cambridge University Press, Cambridge, England, 1972), Chap. 8.

[34]G.-L. Zhao and W. Y. Ching, Phys. Rev. Lett. **62**, 2511 (1989).

[35]P. B. Allen and J. Q. Broughton, J. Phys. Chem. **91**, 4964 (1987).